Reactions of $F^+(^3P)$ and $F^+(^1D)$ with Silicon Oxide. Possibility of Spin-Forbidden Processes

Cristina Trujillo, Al Mokhtar Lamsabhi, Otilia Mó, and Manuel Yáñez*

Departamento de Química, C-9, Universidad Autónoma de Madrid, Cantoblanco, 28049-Madrid, Spain

Received: December 13, 2005; In Final Form: April 5, 2006

High level ab initio and density functional theory calculations have been carried out to study the potential energy surfaces associated with the reactions of F^+ in its ^3P ground state and in its ^1D first excited state with silicon dioxide. The structures and vibrational frequencies of the stationary points of both potential energy surfaces were obtained at the B3LYP/6-31G(d) level. Final energies were calculated at the B3LYP/6-311+G(3df,2p) and at the G3X levels of theory. $[Si, O_2, F]^+$ singlet and triplet state cations present very different bonding characteristics. The most favorable reactions path in $F^+(^3P) + SiO_2$ reactions should yield $O_2 + SiF^+$, while in the reactions in the first excited state, only a charge exchange process, yielding $F(^2P) + SiO_2^+(^2A)$, should be observed. However, both potential energy surfaces cross each other, because although the entrance $F^+(^3P) + SiO_2$ lies 34.5 kcal/mol below $F^+(^1D) + SiO_2$, the global minimum of the singlet PES lies 10.3 kcal/mol below the global minimum of the triplet. The minimum energy crossing point between them is close to the global minimum, and the spin−orbit coupling is not zero, suggesting that very likely some of the products will be formed in the singlet hypersurface. The existence of instabilities and large spin-contamination in the description of some of the systems render the DFT calculations unreliable.

1. Introduction

Gas-phase ion processes are of great relevance in atmospheric and interstellar chemistry.[1−3] It is nowadays well established that ion−molecule reactions seem to be in the origin of the different species detected inside interstellar clouds.[1,3] However, in general, the only information available in most of these processes is the product distribution, but very little is known about the mechanism leading to these products.[4−7] In this respect the role of high-level ab initio molecular orbital techniques[8−13] was of great importance in elucidating these mechanisms.[14−32] Actually, in many occasions, the ab initio or density functional theory calculations are the only alternative available to investigate the structures of ionic species, which, very often, are elusive to experimental observation. Besides, high-level theoretical methods reach the so-called *chemical accuracy*, and therefore, many thermodynamic properties of neutral and charged species can be estimated within ±2.0 kcal/mol of the experimental values, when available.[33−38] High accuracy is important in this field because in interstellar space only exothermic processes are likely to occur, due to the extreme interstellar conditions of low temperature and density, and therefore an accurate knowledge of the topology of the corresponding potential energy surface (PES) is of critical importance.

The aim of this paper is to investigate the gas-phase reactions between F^+ in its ^3P ground state and in its ^1D first excited state and silicon dioxide. SiO_2 is a dominant component of interstellar dust supplied from supernovae,[39−41] and most of the meteorites are SiO_2-rich objects,[42−44] and therefore their ablation when they enter in the Earth atmosphere and in the atmosphere of other planets may be a possible source of atmospheric silicon oxide.

2. Computational Details

The topology of the $[Si, O_2, F]^+$ singlet and triplet PESs was explored through the use of density functional and ab initio methods. The geometries of the different stationary points were optimized using the B3LYP approach together with a 6-31G(d) basis set expansion. This approach has been found to yield reliable structures and frequencies for systems formed by the interaction between monocations and neutral systems[45−50] The B3LYP method includes Becke's three parameter nonlocal hybrid exchange potential[51] and the non-local-correlation functional of Lee, Yang and Parr.[52] Harmonic vibrational frequencies were obtained at the same level of theory to classify the stationary points as local minima or transition states and to estimate the corresponding zero point energies (ZPE), which were scaled by the empirical factor 0.9806.[53] Final energies were obtained by single point B3LYP/6-311+G(3df,2p) calculations on the aforementioned optimized geometries. To assess the reliability of this scheme we have also obtained the final energies of the different stationary points using the G3X theory,[54] which is based on B3LYP/6-31G(d) optimized structures. This theoretical scheme has been proved to be very accurate for a large set of molecules. For triplets, the corresponding unrestricted formalism was used, but in no case was the spin contamination found to be significant, since the S^2 expectation value was always smaller than 2.0004. The final assignment of transition states was done by using the internal reaction coordinate (IRC) procedure as implemented in Gaussian-03.[55]

To locate conical intersections within a given PES or to locate the minimum energy crossing points (MECP) between the singlet and the triplet hypersurfaces we have used a CASSCF(6,6) formalism and the procedure developed by Robb et al.[56] For the latter case, and in order to ensure the reliability of the calculated spin−orbit coupling needed to estimate the probability of intersystem crossing between both surfaces, the CASSCF(6,6) optimized geometry of the MECP was refined by enlarging the active space to 10 electrons and 10 orbitals. The same theoretical scheme was used to calculate the corresponding spin−orbit coupling by means of the method developed by Palmieri et al.[57] Both conical intersections and spin−orbit

10.1021/jp057281n CCC: $33.50
Published on Web 05/10/2006

coupling calculations are carried out using a state average procedure, in which identical weight is assigned to the two states involved. These calculations were carried using MOLPRO suite of programs.[58]

Because of the large recombination energies of both $F^+(^3P)$ and $F^+(^1D)$,[59] the interaction of these cations with the neutral is followed by a drastic reorganization of the charge distribution of the whole system. To adequately describe these effects we have used two different partition techniques, namely the atoms in molecules (AIM) theory[60] and the natural bond orbital (NBO) analysis.[61] The AIM theory is based in a topological analysis of the electron charge density, $\rho(\mathbf{r})$ and its Laplacian, $\nabla^2\rho(\mathbf{r})$. More specifically, we have located the so-called bond critical points (bcps), i.e., points where $\rho(\mathbf{r})$ is minimum along the bond path and maximum in the other two directions. In general the value of ρ at these points provide useful information on the strength of the bond and the ensemble of bcps and the corresponding bond paths permit to define the corresponding molecular graph. The nature of the bonds formed between the ion and the neutral system was analyzed by means of contour maps of the energy density, defined as

$$H(\vec{r}) = (1/4)\nabla^2\rho(\vec{r}) - G(\vec{r})$$

where $\nabla^2\rho(\vec{r})$ and $G(\vec{r})$ are the Laplacian of the electron density and the kinetic energy density, respectively. Bonding regions in which the energy density is negative correspond to covalent linkages.[62,63] Conversely, typical ionic bonds are associated with regions where the energy density is clearly positive.

AIM calculations have been carried out by using the AIMPAC series of programs.[64]

3. Results and Discussion

The different local minima of both PES's were numbered in increasing energy order. In our nomenclature we have used **T** to identify the triplets and **S** to identify the singlets. For the transition states the two digits attached to this symbol identifies the two local minima that are connected by that transition state. The optimized geometries of the different local minima are schematized in Figure 1. The optimized geometries of all the stationary points of both potential energy surfaces are summarized in Table S1 of the Supporting Information.

Structure and Bonding Analysis. A cursory examination of Figure 1 clearly shows significant dissimilarities between the structures of singlets and triplets. In both $F^+(^3P)$, $F^+(^1D) + SiO_2$ reactions the direct association of the halogen cation to the neutral system can take place at the silicon atom, to yield **T1** and **S1** adducts, respectively, or at the oxygen atoms to yield the **T4** and **S4** structures, respectively. In both cases, the former are the global minima of the PES and the latter the less stable complexes, however, there are significant differences in structure and bonding between the members of both couples. As illustrated in Figure 1, **S1** is apparently a cyclic system in which F^+ attachment triggered the formation of a new O−O bond, absent in the neutral system. As a matter of fact, the corresponding molecular graph (see Figure 2) shows the existence of a bcp between both nuclei with a charge density about half that found in the O−O bond of hydrogen peroxide. Conversely, **T1** is an open structure, with an O−O distance of 2.858 Å. This can be understood by taking into account the huge reorganization of the electron distribution of the SiO_2 moiety upon F^+ association. The energy recombination of F^+ is one of the largest within the periodic system, and therefore a complete transfer of at least one electron from the neutral base to the incoming cation takes place. Indeed, our results indicate that in both complexes the net charge of the SiO_2 moiety is +1.2 for the singlet and +1.0 for the triplet. The consequence of this charge transfer from SiO_2 toward F^+ is that the unpaired electrons, initially located on F^+ are now on the two oxygen atoms of the SiO_2 moiety, which in complex **T1** have a spin density of 1.0, preventing the formation of a linkage between both oxygens, since the system has to preserve the overall triplet multiplicity.

It can be similarly observed that while **S4**, is a cyclic symmetric complex, in **T4** the fluorine atom is only bonded to one of the oxygen atoms. The lack of symmetry of **T4** is again imposed by the necessity of preserving the overall triplet multiplicity, since in **T4** the unpaired electrons are located respectively on Si and on one of the oxygen atoms, which therefore cannot be bonded to F. These differences are well reflected in their charge densities. In **T4**, no bcp is found between F and one of the oxygen atoms, while in **S4** both exist, as well as the corresponding ring critical point (See Figure 2).

The minimum **S2** in which the F atom bridges between Si and O, has no equivalent in the triplet hypersurface. In this local minimum, that is connected to the global minimum through the **S12** transition state, Si appears covalently bonded to both oxygens and apparently to the fluorine atom, although no bcp has been located between both atoms, so very likely the relative short distance between Si and F is due to an electrostatic attraction between them (see Figure 2).

The third local minimum in stability order in both PES's correspond to a weakly bound species between O−Si−F^+ and a neutral oxygen atom. As illustrated in Figure 3, the energy density between the oxygen atom and the O−Si−F^+ subunit is positive as it corresponds to an electrostatic interaction between the ion and the oxygen. The only difference between complexes **T3** and **S3** is that in the former the oxygen atom interacting with the O−Si−F^+ fragment is in its ^3P ground state, while in S3 is in its ^1D excited state. Consistently, the energy difference between these two complexes (64.2 kcal mol^{-1}) is practically identical to the gap between $O(^1D)$ and $O(^3P)$ (64.6 kcal mol^{-1}).

G3 vs DFT Results. The profiles of the $F^+(^3P, ^1D) + SiO_2$ reactions are shown in Figures 4 and 5, respectively. It can been seen that in qualitative terms the topology predicted at the G3X level is not significantly different from the one obtained at the B3LYP/6-311+G(3df,2p) level. There are however some significant quantitative differences that need to be commented. Probably the most significant one is the energy gap between $F^+(^1D)$ and $F^+(^3P)$. The G3X calculated value (61.3 kcal mol^{-1}) is in very good agreement with previous theoretical estimates obtained at the G2-level (62.1 kcal mol^{-1})[15,19] as well as with the experimental value (59.7 kcal mol^{-1}).[65] However, the B3LYP/6-311+G(3df,2p) value (83.2 kcal mol^{-1}) dramatically overestimates this energy difference. The reason for this pathological behavior is the RHF−UHF instability of the $F^+(^1D)$ DFT wave function. Furthermore, the problem does not disappear when an unrestricted formalism is used to calculate this singlet state, because the unrestricted wave function is too low in energy and presents a very high spin contamination, and therefore these unrestricted DFT results have no physical meaning as it has been shown before in the literature for other halogen containing systems.[66] This could invalidate the use of this DFT approach for the description of the stationary points of the singlet potential energy surface. However, we have verified that for all $[Si, O_2, F]^+$ singlet-state complexes the wave function does not present any kind of instability. This would explain why, although the relative stabilities of the entrance

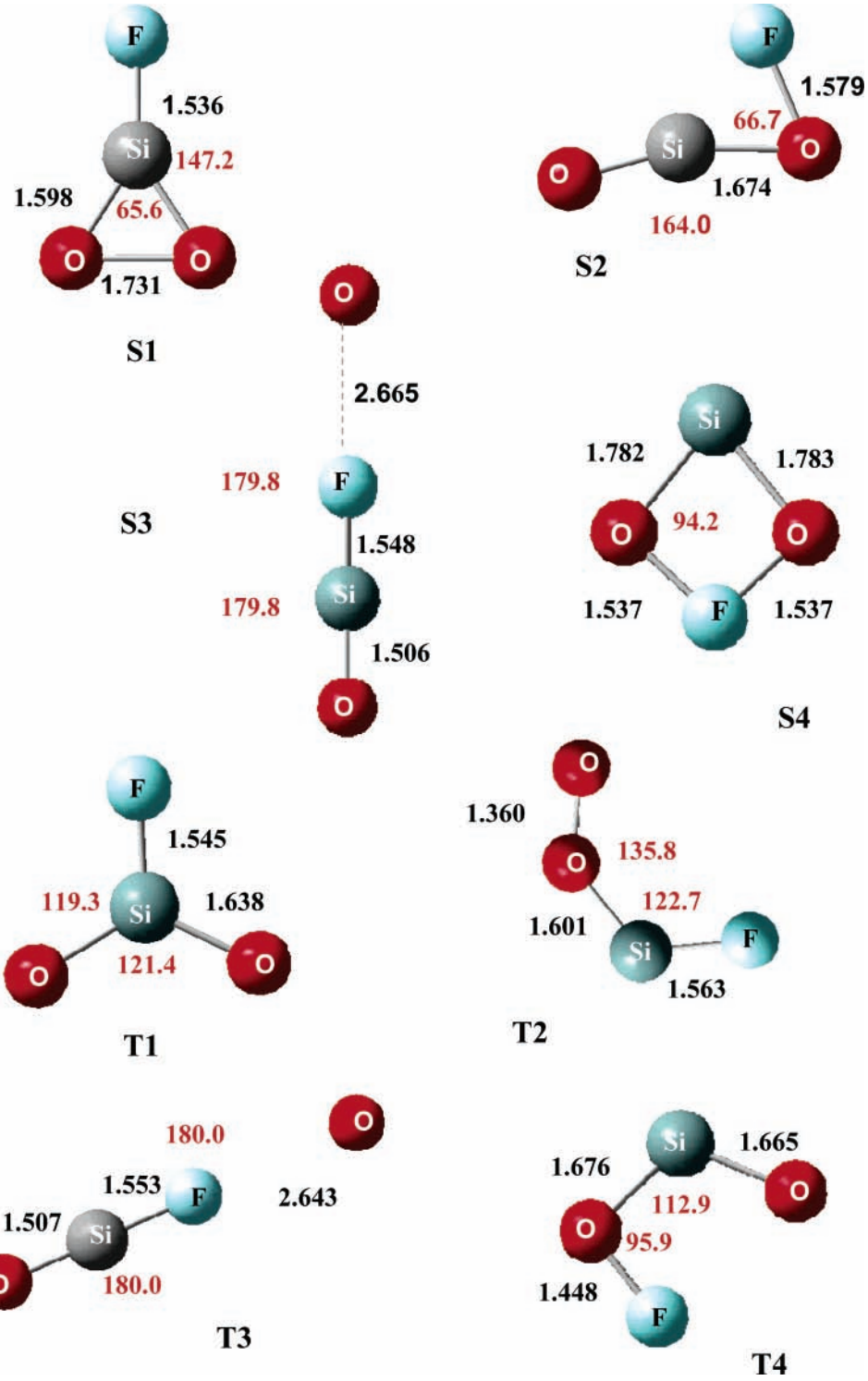

Figure 1. Optimized geometries of the local minima of the singlet and triplet [Si, O_2, F]$^+$ PES's. Bond lengths (in black) are in Å and bond angles (in red) are in deg.

channel is very badly described at the B3LYP level, the relative stabilities of the stationary points of the [Si, O_2, F]$^+$ singlet PES is in reasonably good agreement with those obtained at the G3X level of theory. We have also checked that the B3LYP/6-31G(d) optimized geometries which are in the base of the G3X method do not differ significantly from those obtained at the MP2/6-31G(d) level of theory.

The second important failure of the DFT approach is the relative energy of the exit channel leading to FO + SiO^+, which is predicted to be much lower than the other exit channels, in clear contrast with the G3X estimates. The reason for this disagreement, is that both the DFT wave functions for FO and SiO^+ present internal instabilities. Moreover, any effort to remove these internal instabilities failed, because the resulting wave functions present a very large spin contamination. This pathology affects to both PES and have important consequences because, while at the B3LYP level the most exothermic process in the $F^+(^1D)$ + SiO_2 reaction is that leading to FO + SiO^+, at the G3X level of theory would correspond to the charge exchange process producing F + SiO_2^+. The effect is less dramatic as far as the $F^+(^3P)$ + SiO_2 reaction is concerned, because both theoretical schemes predict as the most exothermic

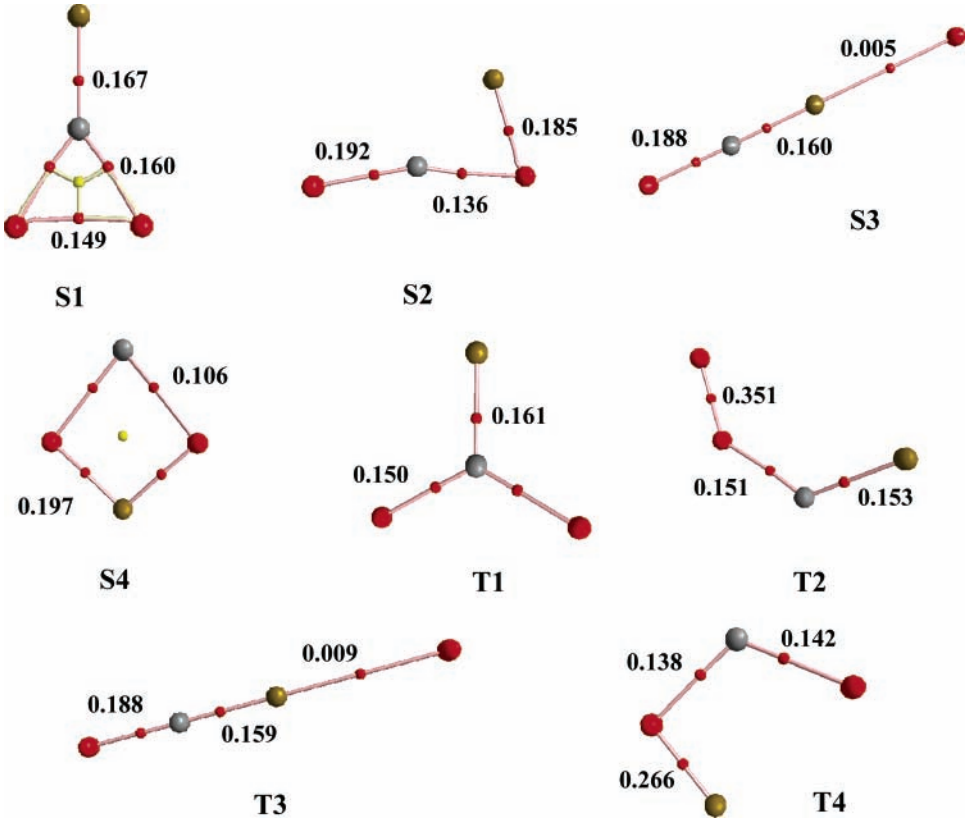

Figure 2. Molecular graphs of the local minima of the singlet and triplet [Si, O_2, F]$^+$ PES's. Charge densities at the bcps (red points) are in e au^{-3}.

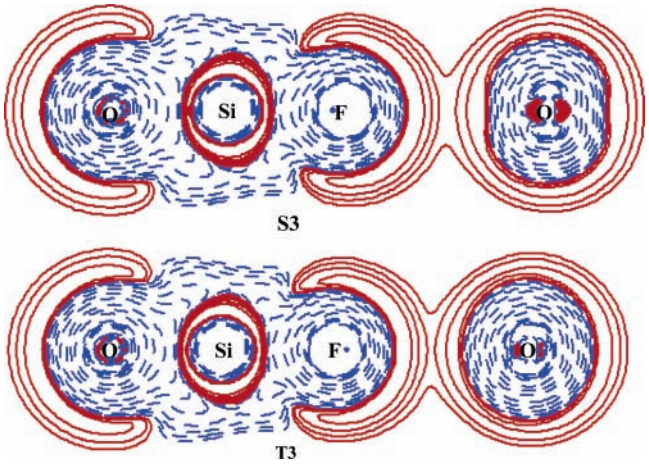

Figure 3. Energy density, H(**r**), contour map for **S3** and **T3** complexes. Blue-dashed lines and solid-red lines correspond to negative and positive values of H(**r**).

process that leading to $SiF^+ + O_2$, and only the highest energy dissociations into $FO + SiO^+$ and $F + SiO_2^+$, appear interchanged.

Taking into account this analysis, in what follows our discussion will be based exclusively on the G3X PES's.

$F^+(^3P)$ + SiO_2 Reactions. It is reasonable to assume that the first step of the $F^+(^3P) + SiO_2$ reaction would be the attachment of the monocation to the most basic center of the neutral, yielding the **T1** complex (see Figure 4). As mentioned in previous sections the SiO_2 moiety undergoes a drastic charge reorganization, not only because of the charge transfer from the neutral to the incoming ion, but also due to the rehybridization of the Si atom. One of the consequences of this electron density redistribution in **T1** is a weakening of the Si−O bonds that lengthen 0.12 Å. This weakening is also reflected in the charge density at the Si−O bcp that decreases significantly on going from the neutral system to **T1** molecular ion. Consistently, the Si−O stretching frequency appears in **T1** 328 cm^{-1} red-shifted with respect to neutral SiO_2. As a consequence the cleavage of one of the Si−O bonds is relatively easy. The oxygen atom detached from **T1** can now migrate toward the oxygen atom of the FSiO subunit, through the **T12** transition state, to yield the local minimum **T2**, or alternatively can interact with the fluorine atom of the aforementioned subunit to yield complex **T3**. The first of these minima, would eventually dissociate into O_2 in its triplet ground state and SiF^+. It can be observed however that this dissociation limit lies lower in energy than the local minimum **T2**, situation that can only be explained if the aforementioned dissociation takes place through an activation barrier. This barrier would exist if this dissociation limit is diabatically correlated with an excited state of **T2**, while **T2** in its ground state would diabatically dissociate to yield $O_2^+ + SiF$, which are higher in energy. As a matter of fact in **T2**, as we have mentioned above, one is on the terminal oxygen and the other one on the Si atom a spin distribution which is compatible with its dissociation into $O_2^+ + SiF$, but not with its dissociation into $O_2 + FSi^+$, because in these products the two unpaired electrons are located on the oxygen molecule. Hence, this dissociation would require a drastic reorganization of the electron distribution through the interaction with the corresponding excited state. The conical intersection associated with the avoided crossing between both diabatic surfaces was located at CASSCF(10,10)/6-31G* level of theory and corresponds to a barrier of 5.2 kcal mol^{-1} above **T2**, and therefore this becomes the most favorable reaction channel with origin in **T1**. This barrier, connects the minimum **T2**, through **TS25**, with a weakly bound complex (**T5**) between the two dissociation fragments O_2 and SiF^+, which lies 6.1 kcal mol^{-1} below the dissociation limit. It is worth mentioning that the dissociation

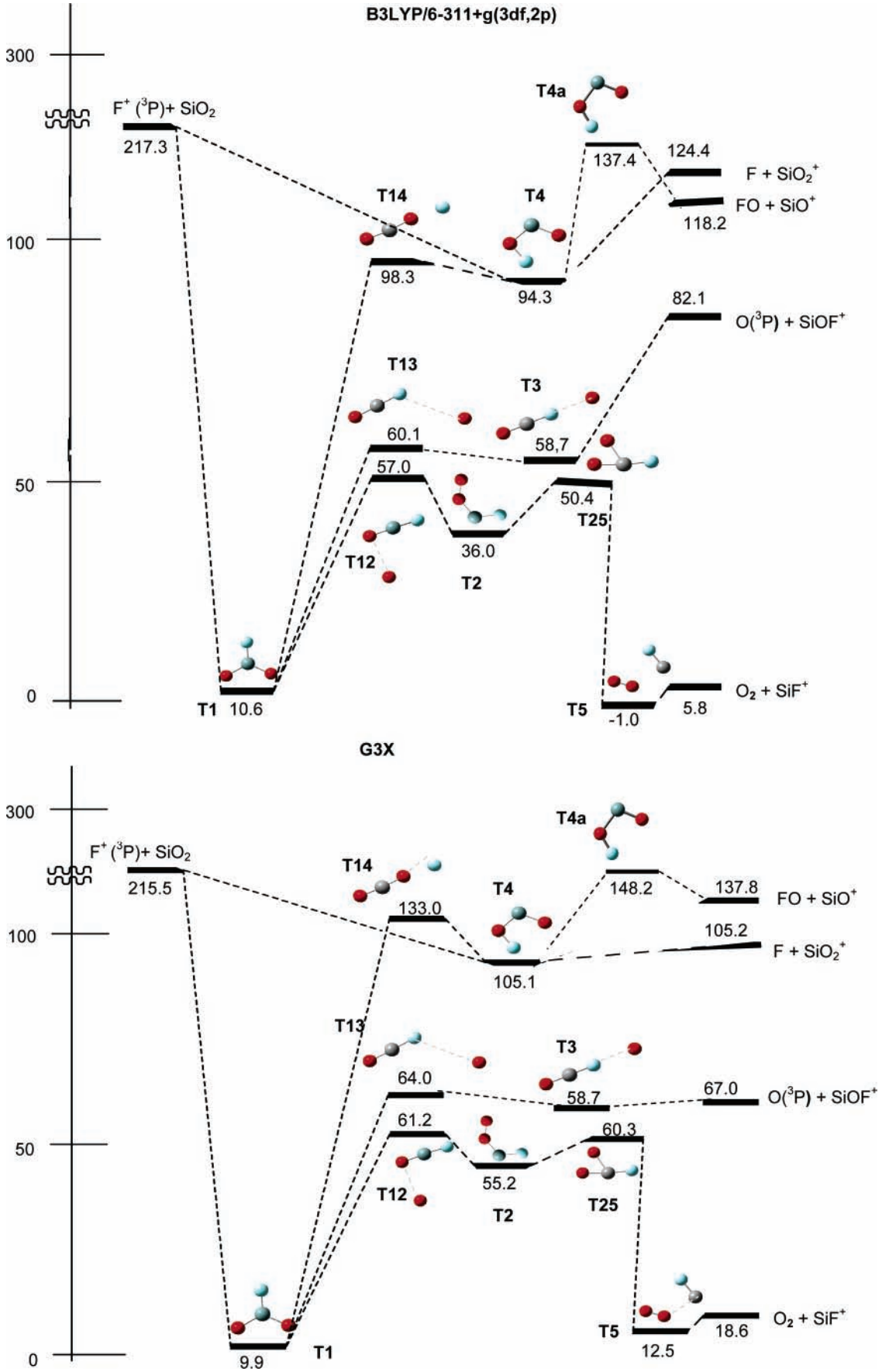

Figure 4. Potential energy profile for the $F^+(^3P) + SiO_2$ gas-phase reactions. Relative energies in kcal mol^{-1} referred to the most stable singlet **S1**. The **TS4a** barrier with respect to **T4** has been estimated by using a CASSCF(6,6) approach.

of **T5** into O_2 and SiF^+ with both products in their triplet states, although spin-allowed should not take place because the corresponding exist channel lies much higher (60.8 kcal mol^{-1}) in energy. **T4** would dissociate diabatically into $F(^2P) + SiO_2^+$,

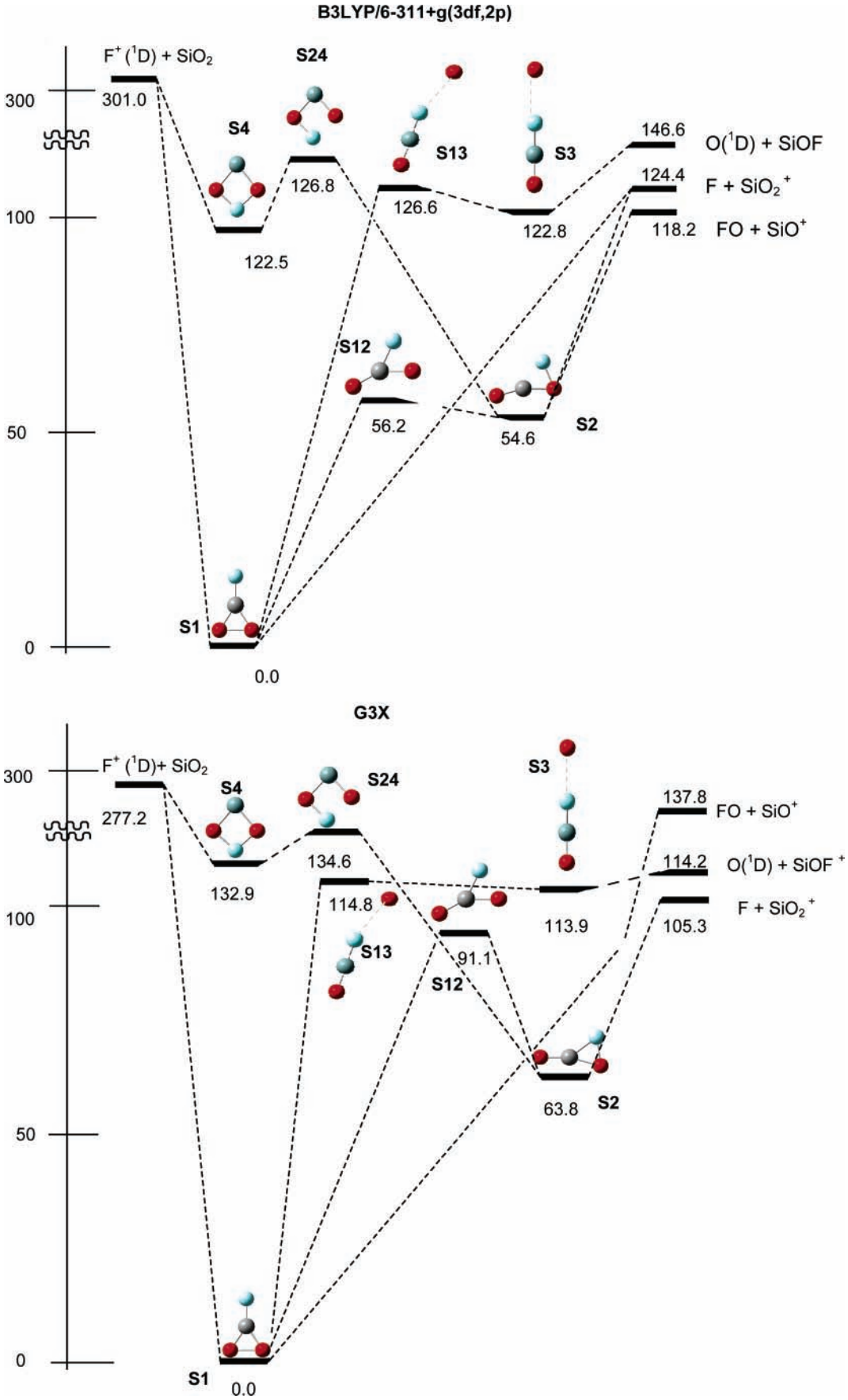

Figure 5. Potential energy profile for the $F^+(^1D) + SiO_2$ gas-phase reactions. Relative energies in kcal mol^{-1} referred to the most stable singlet **S1**.

since a charge transfer occurs already in the formation of this species. However, its dissociation into $FO + SiO^+$ should take place through a conical intersection (**TS4a**) that implies an activation barrier of 43.1 kcal mol^{-1}.

Minimum **T3** will dissociate into $SiOF^+ + O(^3P)$. Since the activation barriers connecting **T1** with **T2** and with **T3** are not very different, the formation of some amount of **T3** cannot be discarded, in principle. Under such assumption $SiOF^+$ would be a secondary product of the $F^+(^3P) + SiO_2$ reaction. The other possible reaction paths with origin in **T1** would lead to a charge exchange process, either directly or through a previous isomerization to yield **T4**, but both processes are not competitive with the isomerizations to yield **T2** and/or **T3**.

$F^+(^1D) + SiO_2$ Reactions. The possible evolution of the singlet global minimum **S1** (see Figure 5), formed also by direct attachment of $F^+(^1D)$ to the neutral base, is markedly different to that discussed above for the corresponding triplet adducts, **T1**, because the exit channel associated with the charge exchange process lies now lower in energy than the dissociation into $SiOF^+ + O(^1D)$, because in this case the oxygen atom is produced in its first excited state. Hence, the most favorable pathway is that leading to the isomer **S2**, which will eventually dissociate into $F + SiO_2^+$. It is worth noting that the global minimum can also directly dissociate to yield the same products. As in the case of the triplets, the cleavage of one of the Si−O bonds is also possible and this would yield to the weakly bound complex **S3**, that would easily dissociate by losing $O(^1D)$. However, this reaction path requires activation barriers higher than the isomerization yielding **S2** and even higher than the direct dissociation of **S1** into $F + SiO_2^+$.

In summary, we can conclude that $F^+ + SiO_2$ reaction in the triplet subspace would yield as dominant products $SiF^+ + O_2$ in a strongly exothermic process, while the same reaction within the singlet manifold should lead preferentially to a charge exchange process.

It is important to note, however, that although the $F^+(^3P) + SiO_2$ entrance channel lies 34.5 kcal mol^{-1} lower in energy than the $F^+(^1D) + SiO_2$ one, the global minimum of the triplet manifold lies 9.9 kcal mol^{-1} higher in energy than the singlet global minimum indicating that both hypersurfaces cross each other at least once. The MECP in the region close to both global minima is, as expected not very far from **T1**. The spin−orbit coupling between both hypersurfaces is estimated at this point to be 1.32 cm^{-1}. This value indicates that the probability of observing spin-forbidden processes, at variance with what has been found for other reactions involving F^+ cations[19] is rather small but not zero. In other words, one should expect some of the flux in the $F^+(^3P) + SiO_2$ reaction to pass to the singlet PES's through the coupling of both hyper-surfaces in the vicinity of the global minimum **T1**, and therefore although the SiF^+ cation should be the dominant product, some SiO_2^+ should also be formed.

Heats of Formation. Since the information available on the heats of formation of molecular ions is very scarce, we have considered it of interest to estimate this magnitude for the main product ion of the reaction, SiF^+. For this purpose we have used the main reactive process

$$F^+(^3P) + SiO_2 \rightarrow SiF^+ + O_2(^3P)$$

which has the advantage of being an isogiric process, that is a process in which the number of unpaired electrons are equal in both sides of the reaction. The reaction enthalpy was estimated at the G3 level of theory and combined with the experimental heats of formation[59] of $F^+(^3P)$, SiO_2, and $O(^3P)$ to obtain an estimate of the heat of formation of SiF^+. The value so obtained was 530 kJ/mol.

Conclusions

The molecular cations formed in the reactions between F^+ in its ^3P ground state differ significantly in their structure and bonding characteristics from those formed in $F^+(^1D) + SiO_2$ reactions, because the bonding in the former is strongly conditioned by the fact that the system has to maintain an overall triplet multiplicity. This has a significant effect in their relative stabilities and although the $F^+(^1D) + SiO_2$ entrance channel lies 34.5 kcal mol^{-1} higher in energy than the corresponding triplet, the singlet global minimum is 9.9 kcal mol^{-1} more stable than the corresponding triplet, because in the latter the O−O bonding found in the former cannot exist.

The topology of both PES's is also significantly different and while for the singlets the most favorable process would correspond to a simple charge exchange, for the triplets the dominant product ion should be SiF^+, although the formation of smaller amounts of $SiOF^+$ cannot be discarded, in principle. The possibility of having spin-forbidden process is not null, since both potential surfaces cross each other in the vicinity of the global minima, and the spin-coupling between them at the corresponding minimum energy crossing point is not zero. However, the coupling is rather small, and therefore one should expect only a small fraction of the initial flux to go from the triplet to the singlet PES, to yield as minor product SiO_2^+. The heat of formation of the dominant product ion, SiF^+ was estimated to be 530 kJ mol^{-1}.

Acknowledgment. This work has been partially supported by the DGES Project No. BQ2003-0894 and by the Project MADRISOLAR. Ref.: S-0505/PPQ/0225 of the Comunidad Autónoma de Madrid. C.T. acknowledges a FPI grant and A.M.L. a postdoctoral Juan de la Cierva contract from the Ministerio de Educación y Ciencia. We also gratefully acknowledge generous allocations of computing time from the Centro de Computación Científica of the Universidad Autónoma de Madrid.

Supporting Information Available: Table containing the optimized geometries (Cartesian coordinates) of the stationary points of the [Si, O_2, F]$^+$ singlet and triplet potential energy surfaces and text giving full versions of refs 55 and 58. This material is available free of charge via the Internet at http://pubs.acs.org.

References and Notes

(1) Duley, W. W.; Williams, D. A. *Interstelar Chemistry*; Academic Press: London, 1984.
(2) Anicich, V. G. J. *J. Phys. Chem. Ref. Data* **1993**, *22*, 1469.
(3) Smith, D.; Spanel, P. *Mass Spectrom. Rev.* **1995**, *14*, 255.
(4) Nicolas, C.; Alcaraz, C.; Thissen, R.; Zabka, J.; Dutuit, O. *Planet., Space Sci.* **2002**, *50*, 877.
(5) Alcaraz, C.; Nicolas, C.; Thissen, R.; Zabka, J.; Dutuit, O. *J. Phys. Chem. A* **2004**, *108*, 9998.
(6) Simon, C.; Lilensten, J.; Dutuit, O.; Thissen, R.; Witasse, O.; Alcaraz, C.; Soldi-Lose, H. *Ann. Geophys*. **2005**, *23*, 781.
(7) Lilensten, J.; Simon, C.; Witasse, O.; Dutuit, O.; Thissen, R.; Alcaraz, C. *Icarus* **2005**, *174*, 285.
(8) Curtiss, L. A.; Raghavachari, K.; Trucks, G. W.; Pople, J. A. *J. Chem. Phys.* **1991**, *94*, 7221.
(9) Petersson, G. A.; Tensfeldt, T. G.; Montgomery, J. A., Jr. *J. Chem. Phys.* **1991**, *94*, 6091.
(10) Curtiss, L. A.; Raghavachari, K.; Redfern, P. C.; Rassolov, V.; Pople, J. A. *J. Chem. Phys.* **1998**, *109*, 7764.
(11) Mayer, P. M.; Parkinson, C. J.; Smith, D. M.; Radom, L. *J. Chem. Phys.* **1998**, *108*, 604.
(12) Montgomery, J. A., Jr.; Frisch, M. J.; Ochterski, J. W.; Peterson, G. A. *J. Chem. Phys.* **1999**, *110*, 2822.
(13) Solling, T. I.; Smith, D. M.; Radom, L.; Freitag, M. A.; Gorodn, M. S. *J. Chem. Phys.* **2001**, *115*, 8758.

(14) Sadygov, R. G.; Yarkony, D. R. *J. Chem. Phys.* **1997**, *107*, 4994.
(15) Manuel, M.; Mó, O.; Yáñez, M. *Mol. Phys.* **1997**, *91*, 503.
(16) Manuel, M.; Mó, O.; Yáñez, M. *J. Phys. Chem. A* **1997**, *101*, 1722.
(17) Cui, Q.; Morokuma, K.; Bowman, J. M.; Klippenstein, S. J. *J. Chem. Phys.* **1999**, *110*, 9469.
(18) Akagi, H.; Yokoyama, A.; Fujimura, Y.; Takayanagi, T. *Chem. Phys. Lett.* **2000**, *324*, 423.
(19) Fernández-Morata, F.; Alcamí, M.; González, L.; Yáñez, M. *J. Phys. Chem. A* **2000**, *104*, 8075.
(20) Hoffmann, M. R.; Schatz, G. C. *J. Chem. Phys.* **2000**, *113*, 9456.
(21) Aschi, M.; Largo, A. *Chem. Phys. Lett.* **2001**, *265*, 251.
(22) Campomanes, P.; Menéndez, I.; Sordo, T. L. *J. Phys. Chem. A* **2001**, *105*, 229.
(23) Ijjaali, F.; El-Mouhtadi, M.; Esseffar, M.; Alcamí, M.; Mó, O.; Yáñez, M. *Phys. Chem. Chem. Phys.* **2001**, *3*, 179.
(24) Flores, J. R.; Estevez, C. M.; Carballeira, L.; Juste, I. P. *J. Phys. Chem. A* **2001**, *105*, 4716.
(25) Peiró-García, J.; Nebot-Gil, I. *J. Phys. Chem. A* **2002**, *106*, 10302.
(26) Gomez, F. J.; Flores, J. R. *J. Phys. Chem. A* **2003**, *107*, 914.
(27) Cimas, A.; Rayon, V. M.; Aschi, M.; Barrientos, C.; Sordo, J. A.; Largo, A. *J. Chem. Phys.* **2005**, *123*, 114312.
(28) Cimas, A.; Rayon, V. M.; Aschi, M.; Barrientos, C.; Sordo, J. A.; Largo, A. *J. Phys. Chem. A* **2005**, *109*, 6540.
(29) Flores, J. R.; Perez-Juste, I.; Carballeira, L. *Chem. Phys.* **2005**, *313*, 1.
(30) Li, Y. M.; Francisco, J. S. *J. Am. Chem. Soc.* **2005**, *127*, 12144.
(31) Francisco, J. S.; Lyons, J. R.; Williams, I. H. *J. Chem. Phys.* **2005**, *123*, 054302.
(32) Yu, H. G.; Muckerman, J. T.; Francisco, J. S. *J. Phys. Chem. A* **2005**, *109*, 5230.
(33) Curtiss, L. A.; Redfern, P. C.; Raghavachari, K.; Pople, J. A. *J. Chem. Phys.* **1998**, *109*, 42.
(34) Petersson, G. A.; Malick, D. K.; Wilson, W. G.; W.; O. J.; Montgomery Jr, J. A.; Frisch, M. J. *J. Chem. Phys.* **1998**, *109*, 10570.
(35) Curtiss, L. A. R.; K.; Redfern, P. C.; Stefanov, B. B. *J. Chem. Phys.* **1998**, *108*, 692.
(36) Curtiss, L. A.; Redfern, P. C.; Frurip, D. J. *Rev. Comput. Chem.* **2000**, *15*, 147.
(37) Curtiss, L. A.; Raghavachari, K.; Redfern, P. C.; Pople, J. A. *J. Chem. Phys.* **2000**, *112*, 7374.
(38) Redfern, P. C.; Zapol, P.; Curtiss, L. A.; Raghavachari, K. *J. Phys. Chem. A* **2000**, *104*, 5850.
(39) Li, A.; Draine, B. T. *Astrophys. J.* **2002**, *564*, 803.
(40) Schneider, R.; Ferrara, A.; Salvaterra, R. *Mon. Not. R. Astron. Soc.* **2004**, *351*, 1379.
(41) Hirashita, H.; Nozawa, T.; Kozasa, T.; Ishii, T. T.; Takeuchi, T. T. *Mon. Not. R. Astron. Soc.* **2005**, *357*, 1077.
(42) Horz, F.; Mittlefehldt, D. W.; See, T. H.; Galindo, C. *Meteor., Planet Sci.* **2002**, *37*, 501.
(43) Murty, S. V. S.; Rai, V. K.; Shukla, A. D.; Srinivasan, G.; Shukla, P. N.; Suthar, K. M.; Bhandari, N.; Bischoff, A. *Meteor., Planet Sci.* **2004**, *39*, 387.
(44) Simon, S. B.; Grossman, L. *Geochim. Cosmochim. Acta* **2004**, *68*, 4237.
(45) Bertrán, J.; Rodríguez-Santiago, L.; Sodupe, M. *J. Phys. Chem. B* **1999**, *103*, 2310.
(46) Luna, A.; Alcamí, M.; Mó, O.; Yáñez, M. *Chem. Phys. Lett.* **2000**, *320*, 129.
(47) Alcamí, M.; Mó, O.; Yáñez, M. *Mass Spectrom. Rev.* **2001**, *20*, 195.
(48) Boutreau, L.; Toulhoat, P.; Tortajada, J.; Luna, A.; Mó, O.; Yáñez, M. *J. Phys. Chem. A* **2002**, *106*, 9359.
(49) Burk, P.; Koppel, I. A.; Koppel, I.; Kurg, R.; Gal, J.-F.; Maria, P.-C.; Herreros, M.; Notario, R.; Abboud, J.-L. M.; Anvia, F.; Taft, R. W. *J. Phys. Chem. A* **2000**, *104*, 2824.
(50) Gal, J.-F.; Maria, P.-C.; Decouzon, M.; Mó, O.; Yáñez, M. *Int. J. Mass Spectrom.* **2002**, *219*, 445.
(51) Becke, A. D. *J. Chem. Phys.* **1993**, *98*, 1372.
(52) Lee, C.; Yang, W.; Parr, R. G. *Phys. Rev. B* **1988**, *37*, 785.
(53) Scott, A. P.; Radom, L. *J. Phys. Chem.* **1996**, *100*, 16502.
(54) Curtiss, L. A.; Redfern, P. C.; Raghavachari, K.; Pople, J. A. *J. Chem. Phys.* **2001**, *114*, 108.
(55) Frisch, M. J.; et al. Gaussian03, Revision C.02 ed.; Gaussian, Inc.: Wallingford, CT, 2003.
(56) Bearpark, M. J.; Robb, M. A.; Schlegel, H. B. *Chem. Phys. Lett.* **1994**, *223*, 269.
(57) A. Berning; M. Schweizer; H.-J. Werner; P. Knowles; Palmieri, P. *Mol. Phys.* **1998**, *21*, 1823.
(58) Adamos, R. D. et al. Molpro, 2002.6, 2003.
(59) *NIST Chemistry Webbook. Standard Reference Database Number 69. July 2001 Release*; 2001.
(60) Bader, R. F. W. *Atoms In Molecules: A Quantum Theory*; Clarendon Press: Oxford, U.K., 1990.
(61) Reed, A. E.; Curtiss, L. A.; Weinhold, F. *Chem. Rev.* **1988**, *88*, 899.
(62) Alcamí, M.; Luna, A.; Mó, O.; Yáñez, M.; Boutreau, L.; Tortajada, J. *J. Phys. Chem. A* **2002**, *106*, 2641.
(63) Corral, I.; Mó, O.; Yáñez, M. *J. Phys. Chem. A* **2003**, *107*, 1370.
(64) Bader, R. F. W.; Cheeseman, J. R. AIMPAC Program, 2000.
(65) Moore, C. E. *Atomic Energy Levels*; National Bureau of Standards (U.S.): Washington, DC, 1971; Vol. I.
(66) Alcamí, M.; Mó, O.; Yáñez, M.; Cooper, I. L. *J. Chem. Phys.* **2000**, *112*, 6131.